Technische Universität Darmstadt

Fachbereich 20 Informatik

Fachgebiet Simulation und Systemoptimierung

Prof. Dr. Oskar von Stryk

Bachelor Thesis

Martin Bernasconi

Analysis and implementation of a three-dimensional foot model for a biodynamical MBS simulation

Betreuer: Dipl.-Tech. Math. Maximilian Stelzer

Darmstadt, den 10.04.2006

Statutory declaration

Hereby I assure that I wrote independently this present bachelor thesis and did not use any different than the indicated sources and aids.

Darmstadt, 10. Apr. 2006 Signatur

Abstract

This bachelor thesis deals with the investigation of several foot models, which were developed for MBS simulations and researches of human locomotion. The internet was predominantly used for this. Four single models – as presented in the papers – will be introduced and will be rated briefly according to their adaptability and efficiency in the existing MBS–program at the TU Darmstadt. Later, an implementation of the best foot model will be presented.

Index

Symbols and short notations

Latin letters

Symbol	Unit	Term
a	$\frac{m}{s^2}$	acceleration
A	cm^2	area
d, D	cm	diameter
E	Nm, Joule	energy
F	N	force
p	$\frac{N}{mm^2}$	pressure
v	$\frac{m}{s}$	velocity
W	Joule	work

Greek letters

Symbol	Unit	Term
φ	°, rad	angle of rotation
θ	kgm^2	mass moment of inertia

Indices

Symbol	Term
0	start position
max	maximal
mech	mechanical
N	normal
rad	radiant
red	reduced
reib	friction
res	resulting
rot	rotatory
trans	translativ

Short notations

Short notation	Term
1T	first tarsometatarsel joint
2T	second tarsometatarsel joint
3T	third tarsometatarsel joint
4T	fourth tarsometatarsel joint
5T	fifth tarsometatarsel joint
ABA	Articulated Body Algorithm
CP	centre of pressure
DOF	Degree of freedom
GRF	ground reaction force
COS	coordinate system
MP	metatarsophal-angeal
MBS	multi-body system
TC	talocrural
TCN	talocalcaneal
TT	transverse tarsal

Figure index

Table index

1 Introduction

Ever since the nineteen sixties researchers have been busy to simulate human locomotion. The researched movements include athletic (e.g. pole vault, hurdle race) and every-day activities (e.g. moving on stairs, walking). There are several different motivations behind these studies. Simulations can represent natural processes, can make the interior complex structure understandable, and at last optimize the process e.g. with respect to the costs of energy or load of bones.

The knowledge gained is relevant for faculties of sport (increase of performance by perfect locomotion regarding individual body conditions) and medical research, e.g. for the therapy of deficits of locomotion or the development of better artificial limbs by electric muscle stimulation (neuroprothetic).

Another interested party is robotics. The implementation of stable kinds of moving for two-legged robots is a necessity to be able to build robots in future, which act as service robots or creep through holes and perhaps climb to rescue people in life-threatening situations (e.g. in factories contaminated chemically or by radiation). "Also the fact that legs can be used more flexibly in uneven [or] unknown ground, where wheels or chains would fail, plays an important role for the development of walking machines." **[02] [translation by author]**

To simulate moving on legs the (mathematical) model needs the possibility of contact with the ground. This task is performed by the foot. It belongs to the more complex parts of body regarding its interior structure and way of function. Because of this complexity, it is expensive to represent mathematically with all details. Due to the different intentions of foot-studies, several foot models were developed (first in 2, in recent also 3 dimensions). The fundamental simulation methods are FEM and MBS. One of the advantages of the Finite Elements Method is that damper/spring properties can be calculated more exactly. However, FEM is too expensive in computation and not useful to depict a 3-dimensional motion of a whole human body. It is more sensible for a locomotion study, which does not the aim at calculating deformations to use Multi Body Simulation.

Also, the model of a human body on the TUD will be available as MBS model. Therefore I will rate the following foot models with respect to this aspect.

2 Requirements

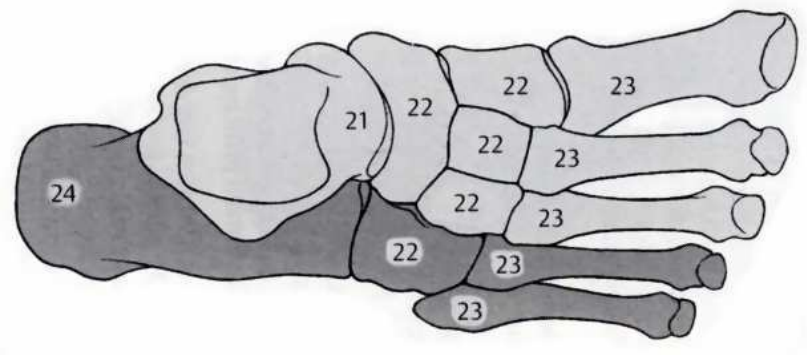

*Fig. 2.1 foot segments of the human body; the most important segments are: 21. talus, 22. middle-foot-bones, 23. metatarsals, 24. calcaneus (from **[06]**)*

I will briefly state the criteria on which I will evaluate the foot models at hand. Foot models, which are restricted to two-dimensional representations, will be left out because we ware aiming at a three-dimensional model. They were created because of their low complexity, low computational costs of the equations and the problem of controlling multisegmental models. Furthermore, the model must be adaptive to the Articulated Body Algorithm. Therefore, it should consist of rigid segments, joints and flexible muscles. Finally, the foot will be used to carry a virtual human being and to simulate ground reaction close to the reality. For that reason I also set a value on the digital foot segment model coming close enough to the real human foot structure (Figure 2.1).

3 The foot models

3.1 Gilchrist and Winter (1996)

One of the more recent models, similar to Meglan's model (1991, 1992), is the one of Gilchrist and Winter (1996) **[01]**. Their idea was to use an alternative set-up to MBS models that represents the spring/damper properties of the plantar surface as well as possible. Nine simple spring/damper systems are used to control a two-part, three-dimensional foot. The two rigid segments are connected by a passive revolute joint. Viscoelastic elements at the foot/floor interface are utilized to allow an external reaction force to develop during the contraction phase. Thereby the heel contact phase can be successfully modelled and the need to fasten the foot to the ground can be avoided.

On the other hand an anatomical skeleton is missing. Therefore, this model appears unusable to measure the load of bones inside the foot, which is one aim of the MBS simulation. I think that in future Gilchrist's and Winter's idea will become more interesting when it will be combined mathematically with a skeleton model.

3.2 Günther (1997)

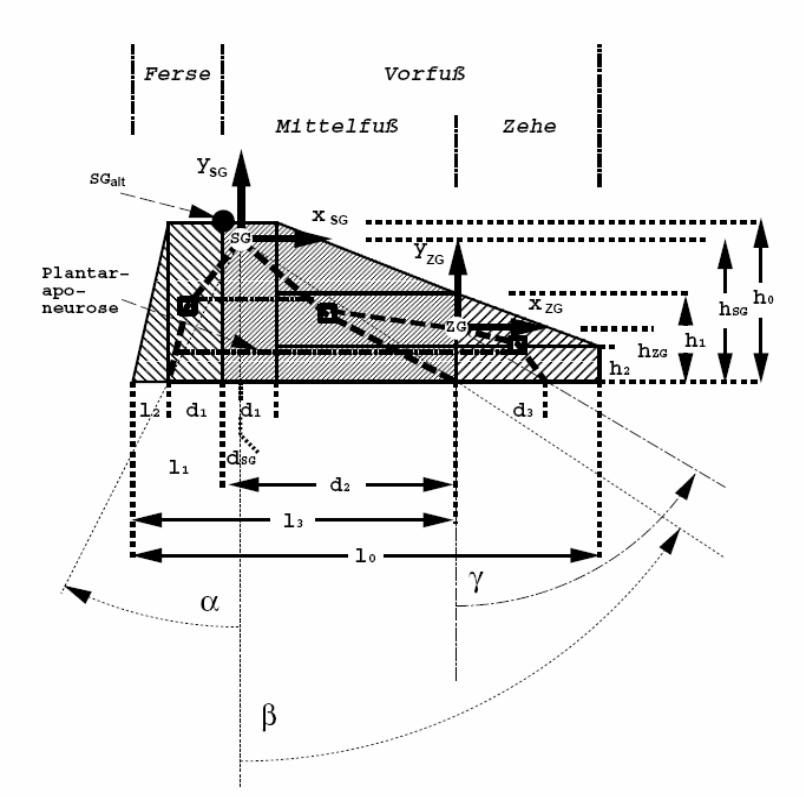

*Fig. 3.2.1 foot model by Günther, 2-dim. lateral view (from **[02]**)*

The next model is by M. Günther (1997) **[02]** [Figure 3.2.1]. He developed it based on papers of Hicks (1954, 1955, 1956). It consists of just three segments (heel, middle-foot, toes), which interact like a braced beam. There are two contact points of force, one on the heel, another on the ball. The rotation of the foot is guaranteed by the hinge-like ankle joint. The hinge-like toe joint admits rotation of the toe segment. Thereby the plantaraponeurosis can be stretched and is in this successfully simulated.

Only the most important force connections for walking (inside the foot) are considered since the main point of his dissertation is to simulate the human gait as a whole, which also explains the small number of segments. For the future, when more complex models are used for even simpler studies thanks to more computing power, I regard this model as a too inaccurate one, because e.g. the forefoot is divided into just two parts. Thereby, keeping the balance by the 1st toe is not considered. Torsion of the heel by the TCN-axis is neglected as well.

3.3 Morlock (1989)

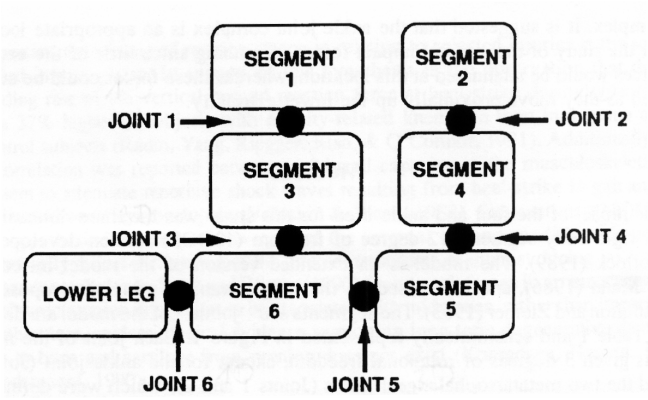

*Fig. 3.3.1 schematic foot model by Morlock (from **[05]**)*

Another foot model was developed by Morlock (1989) **[05]** [Figure 3.3.1]. The six rigid segments are connected by six joints, of which joint number 3, 4, and 5 have three DOFs and joint number 1, 2, and 6 one DOF. These twelve DOFs and six joints simulate altogether ten of the twenty-seven muscles as well as the plantaraponeurosis. The model is based on the weight transfer principle proposed by Hamilton and Ziemer (1983).

It approaches theoretically the anatomical structure of the human foot very well, but it is a schematic foot model. Therefore it would be difficult to extract an anatomical foot model out of the mathematical connections of the imaginary joints.

3.4 Scott and Winter (1993)

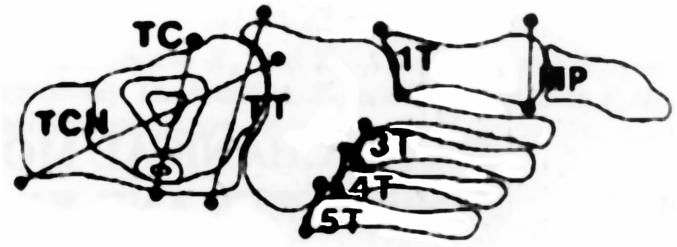

*Fig. 3.4.1 foot model by Scott and Winter, dorsal view (from **[09]**)*

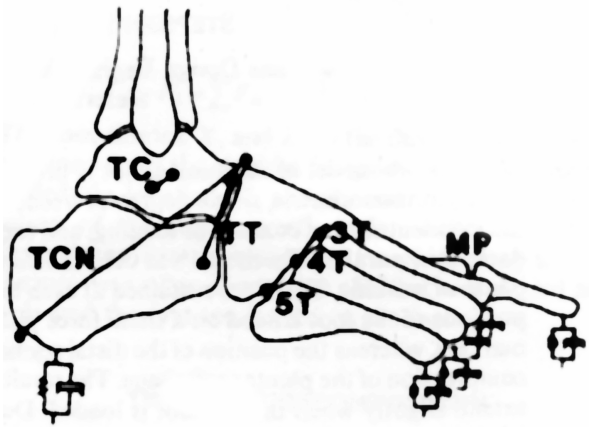

*Fig. 3.4.2 foot model by Scott and Winter, lateral view. (from **[09]**)*
The seventh spring and damper, under the head of the first metatarsal, is obscured.

The last foot model studied is by Scott and Winter (1993) **[09]** [Figure 3.4.1 & 3.4.2]. The model consists of eight rigid segments, which are connected by eight joints with one DOF each. To simulate the ground reaction force, the plantar soft tissue is divided in seven independent sites of contact, each modelled as a nonlinear spring and a nonlinear damper in-parallel. “The talocrural (ankle, TC) joint provides rotation between the talus and the leg, and the talocalcaneal (subtalar, TCN) joint provides rotation between the talus and the calcaneus.” [09] The possibility to represent the angular motion of the talocalcaneal joint adequately by a 1-DOF, monocentric joint was shown by Scott and Winter (1991) **[08]**. “Motion between the hind- and mid-foot regions occurs at the transverse tarsal (mid-tarsal, TT) joint.” [09]

The model assumes that the first, third, fourth, and fifth metatarsal bones have independent motion from the mid-tarsal segment. “[This] independence between the metatarsal bones is necessary to allow all of the metatarsal heads to maintain contact with the ground in order to transmit force when the heel is raised and to produce forefoot twist.” However, the second is attached rigidly with the middle-foot-bones. “This attachment is necessary to allow kinematics of the transverse tarsal [axis] to be collected.” [09]

This model is ideal for the ABA since it consists of rigid segments and joints. In addition it provides the possibility to integrate muscles. Furthermore, it is very strongly oriented towards the anatomy of the human foot. Especially the introduction of the 1st toe seems very interesting to me, because medical tests showed that it plays an important role for keeping the balance. I have used this model for the following paper and will go deeper into the model and especially into its implementation in the next chapter.

4 The implemented model

The data needed for the ABA is in detail (with its program IDs):

- forces and moments of the basis
- for each segment
    - vector to the next segment (.l), i.e. from segment to segment
    - vector to the own centre of gravity (.lC)
    - mass (.mass)
    - inertia tensor
- for each joint
    - rotation axis (.axis)
    - angle of rotation (.angle)
    - angular velocity (.dangle)
    - torque (.u), substituted muscles
- ground recation forces

The ABA regards just a fixed moment. Therefore, all changing values should be continuous rather than discrete, to guarantee temporal independence. These are angle of rotation, angular velocity, torque, and GRFs.

For the following document I will just consider a right human foot.

4.1 Vectors to the next segment and to the center of gravity

For the vectors to the next segment Scott and Winter are oriented towards Salathé et al. **[07]**. The joint positions for the midfoot- and metatarsalbones - as described there - are stated with reference to coordinate systems (x_j, y_j), j = 1-5. Hereby, the x-axis passes trough the contact points of the heel and the respective metatarsal-head, the y-axis perpendicularly through the point of load on the talus. The positions are then given by two matrices, where the rows correspond to the joints and the columns to the metatarsals (all values in cm).

$$A_x = \begin{pmatrix} 13.71 & 14.61 & 13.95 & 12.66 & 11.80 \\ 7.70 & 7.14 & 6.99 & 5.77 & 5.07 \\ 4.49 & 5.26 & 4.87 & 2.48 & 2.48 \\ 3.44 & 3.44 & 3.44 & & \end{pmatrix}, \qquad A_y = \begin{pmatrix} 0 & 0 & 0 & 0 & 0 \\ 3.40 & 3.31 & 3.06 & 2.34 & 2.06 \\ 3.63 & 3.73 & 3.59 & 3.32 & 3.32 \\ 4.55 & 4.55 & 4.55 & & \end{pmatrix}$$

Given the fact that the z-coordinates of the metatarsal heads are 0, 2.60, 4.32, 5.76 and 6.92, the positions of the joint 1T – 5T are as plotted in figure 4.1.1. For these z-values the z-axis of the system (x_1, y_1) was used. The length of the 1st toe was estimated at 6.00 cm according to pictures of Scott and Winter and Werner Platzer **[06]** as well as own measuring.

One should pay attention to the fact that the implemented model uses different coordinate axes than Salathé et al. The z-axis will be directed towards gravity. Hence, for simplification these KOS (x_1, y_1, z) will be used for all coordinates and orientation of axes.

For the remaining joint positions in figure 4.1.1 between leg / talus, talus / calcaneus and talus / middle-foot segment there is no data available, neither from Salathé et al. nor from Scott and Winter. But since the connection point must be on the respective rotation axes (TC, TT, TCN), the connection point on the TC- (green) and TT-axis (blue) is the respective centre of the axis, whereas the connection point on the TCN-axis divides it at a ratio of 1 to 1.9 (measured off pictures of Scott and Winter). The contact point of the TC-axis was used as suspension point for the basis of the model.

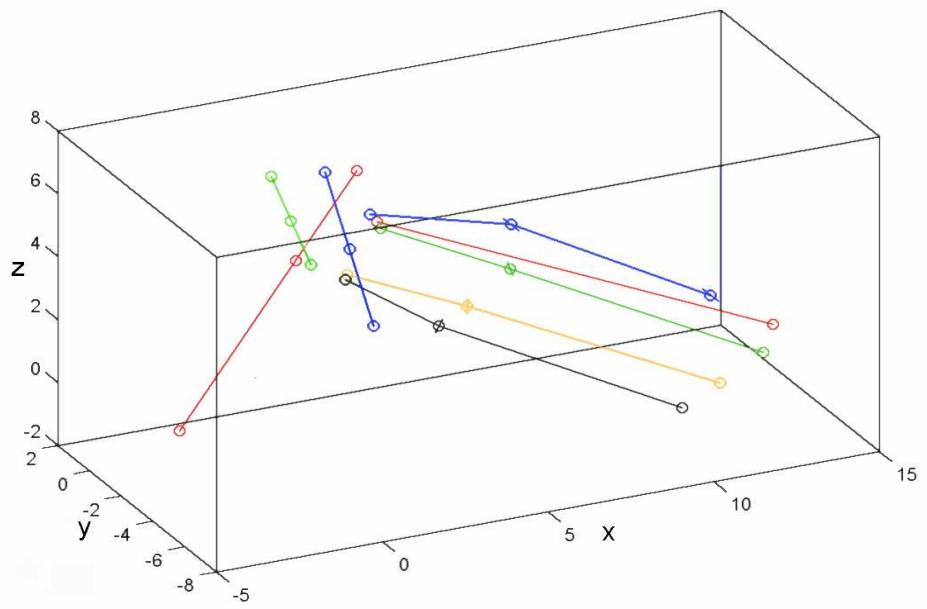

Fig. 4.1.1 coordinates of the joints by Salathé et al. and Scott and Winter

Salathé et al. specifies inside and outside radii for the distinct metatarsal bones. For our model they were approximated by hollow cylinders. Therefore, the vectors to the centre of gravity are half the vectors to the contact point with the ground. Alike we proceed with the 1st toe, the inside and outside radius of which are adopted from the 1st metatarsal bone. The other segments (talus, calcaneus, middle-foot-bones) were approximated by estimated cuboids due to missing geometric data. For this purpose, anatomical pictures of Werner Platzer were used preponderantly. For that reason, the centres of gravity and inertia tensors of the segments are those of the cuboids. Platzer's pictures with the approximating cuboids is shown in figure 4.1.2. Here, all cuboids (in initial position) form an off-z-axis angle of 20°, the talus- and the middle-foot-bone-cuboids an off-y-axis angle of 20°, as well as the calcaneus cuboid an off-y-axis angle of 10°. The supposed metrics are listed in table 4.1.1.

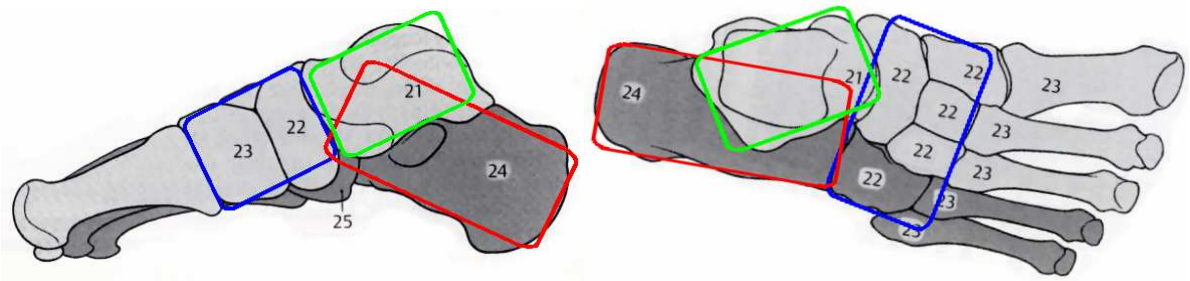

*Fig. 4.1.2 position of the approximated segments (from **[06]**)*

Table 4.1.1 estimated measures of the approximating cuboids

	Talus	Calcaneus	Middle foot segment
length (cm)	5,5	8,0	4,0
width (cm)	4,0	4,0	5,7
height (cm)	3,2	4,0	3,2

4.2 Mass and inertia tensors

Günther's dissertation was used for estimating the masses of the distinct bone segments. He used NASA-data for evaluating the masses of heel, middle foot, and toes. These mass blocks were converted into masses for Scott and Winter's foot model. Masses for the calcaneus, talus, middle foot as a whole (the mass of the second metatarsal bone was added), for each metatarsal bone (the mass of the small toe bone was added) and the masses for each small toe bone, where their two to three bones were summed up to one mass. Günther supplies masses for the heel, middle foot and toes regarding his own foot model. From these three masses three new masses were calculated, one for the talus / calcaneus (0.4 kg), one for the middle foot / metatarsal bones (0.4 kg), and one for the toe bones (0.17 kg) regarding Scott and Winter's model.

The distribution factors, which distribute the three new masses to the searched segments (listed above), were estimated for the metatarsal bones by their volume, those for the remaining segments by pictures. Salathé et al. give inside and outside radii for the metatarsal bones at several points on the bone. Theses values were averaged because these bones will be approximated as hollow cylinders. The lengths of the metatarsal bones are given as well. The values are listed in table 4.2.1.

Table 4.2.1 Values for metatarsalbones

Metatarsal bones	1	2	3	4	5
outside radius (cm)	1,73	1,22	1,14	1,07	1,08
inside radius (cm)	1,53	1,02	0,94	0,87	0,88
length (cm)	5,90	7,20	7,00	7,00	6,90

The estimated distribution factors and resulting masses are listed in table 4.2.2. Here, the segment masses in a row are added up as described above. The factors of [talus, calcaneus], [middle foot bones, metatarsals] and [toes] each add up to 1.

Table 4.2.2 factors for the distribution of mass and final mass

Segment	Factor	Mass (kg)
Talus	0,33	0,132
Fersenknochen	0,67	0,268
Middle foot bones	0,50	0,20
+ 2. metatarsal bone	0,10	0,04
+ 2. toe bone	0,19	0,0323
		0,2723
1. metatarsal bone	0,165	0,066
1. toe bone	0,30	0,051
3. metatarsal bone	0,085	0,034
+ 3. toe bone	0,19	0,0323
		0,0663
4. metatarsal bone	0,075	0,03
+ 4. toe bone	0,19	0,0323
		0,0623
5. metatarsal bone	0,075	0,03
+ 5. toe bone	0,13	0,0221
		0,0521

The metatarsal bones and the 1st toe are approximated as hollow cylinders, talus, calcaneus and middle-foot-bones as homogeneous cuboids, as described in chapter 4.1. The inertia tensors in table 4.2.3, rounded to three post-decimal positions, result from the values in tables 4.1.1 and 4.2.1

Table 4.2.3 inertia tensors of all segments

Segment	x-axis	y-axis	z-axis
Talus	0,288	0,445	0,509
Calcaneus	0,715	1,786	1,786
Middle foot bones	0,712	0,437	0,808
+ 2. metatarsal bone	0,091	0,358	0,358
+ Steinerglieder	0,155	1,739	1,588
total	0,958	2,534	2,754
1. metatarsal bone	0,176	0,279	0,279
1. toe bone	0,136	0,221	0,221
3. metatarsal bone	0,072	0,307	0,307
4. metatarsal bone	0,059	0,284	0,284
5. metatarsal bone	0,051	0,232	0,232

4.3 Axes of rotation of the joints

For the metatarsal bone joints Scott and Winter aligned the x-axis for each joint KOS with the long axis of the following segment. Then, the z-axis was aligned with the respective joint axis. The orientation of the TT-, TC-, and TCN-axes was calculated from two sources. The respective two axes were averaged to avoid major errors concerning the orientation of the axis for the implemented model.

Scott and Winter aligned the rotation-axis of the TT-joint with the talonavicular and calcaneocuboid joints. With this indication, a linear regression with Salathés points induced the first solution, an approximation of Scott and Winter's pictures the second.

The orientation of the TC-, as well as the TCN-axis, is described in a short presentation **[10]**. According to this, the TC-rotation-axis is a line between the two malleoli. Since more precise information could not be found, the locations of the two malleoli were measured at a foot from outside, which correspond with a tolerance of ± 2mm to the length of Salathés foot (Figure 4.3.1). The result of this measurement induced the first solution, an approximation of Scott and Winter's pictures the second.

The data about the orientation of the TCN-axis from the presentation (Figure 4.3.2) were used as the one solution, an approximation of Scott and Winter's pictures the other. The locations of all calculated axes are plotted with Matlab in figure 4.3.3 (see also figure 4.1.1).

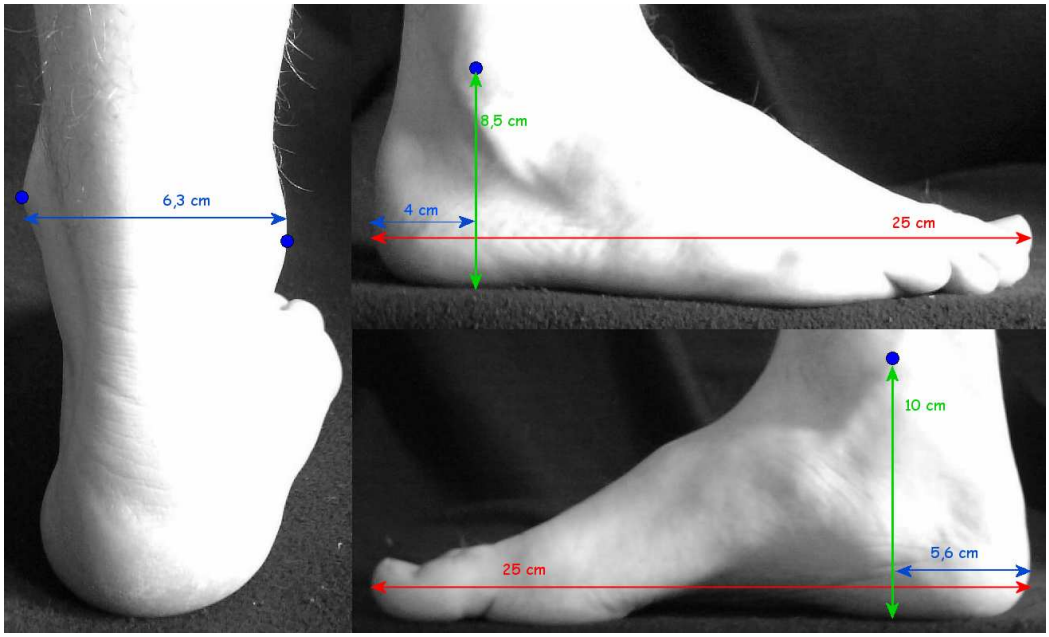

Fig. 4.3.1 coordinates of the malleoli of a human foot

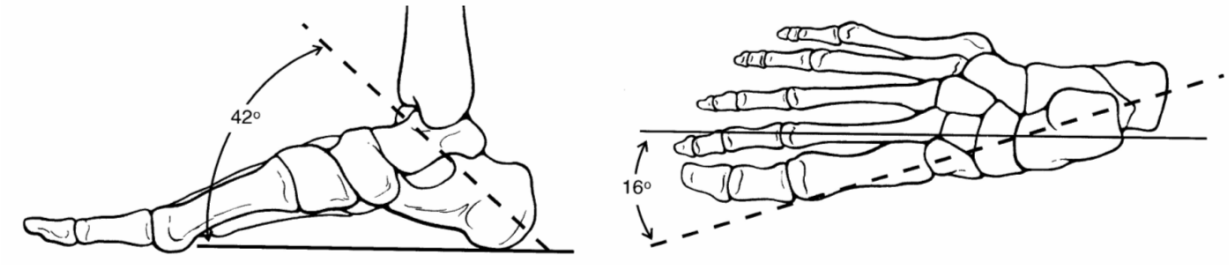

*Fig. 4.3.2 orientation of the TCN-axis (from**[10]**)*

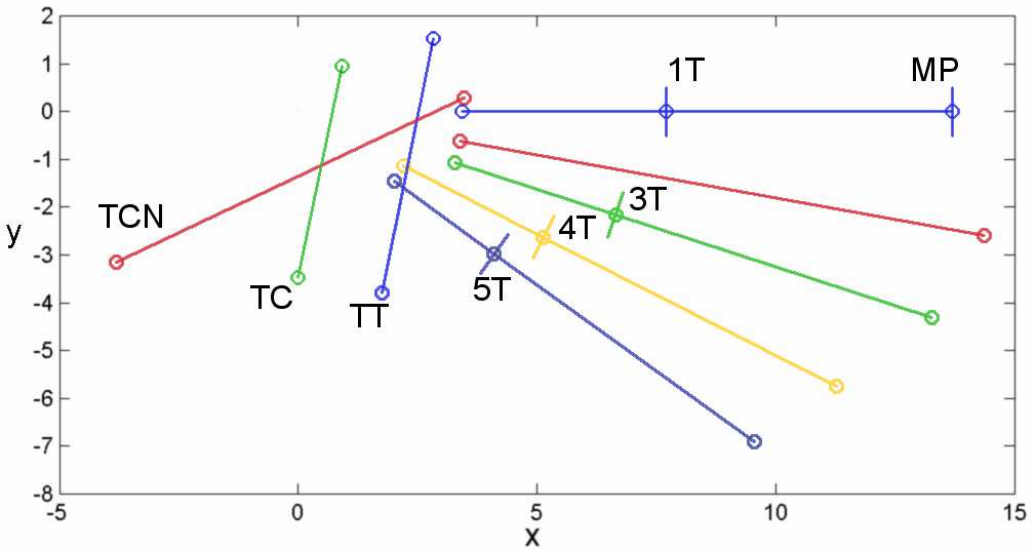

Fig. 4.3.3 orientation of the TT-, TC-, TCN-, 1T-, 3T-, 4T-, 5T- und MP-axes

4.4 Angular of rotation, angular velocity, torque

In their paper from 1991 **[08]**, Scott and Winter present rotation and moment graphs for the TC and TCN joint, in their paper from 1993 for the TT, 1T, 3T, 4T, 5T and MP joints. The x-axis of these graphs labels percent values from 0% - 100%. Here, 0% means the first contact between foot and ground (with the heel) and 100% the leaving of the ground (with the 1st toe). These graphs were scanned and were interpolated by cubic splines with Matlab. Therefore, the resulting graphs are $\in \mathcal{C}^2$. The function for evaluation of the splines was extended, such that the return value is null, if the point to be valuated is smaller than the first or greater than the last supporting point. This extension makes sense e.g. for the rotation graphs, which starts at 13-20% and break off at 83-93%.

The functions of angular velocity were calculated by derivation of the splines of the angle of rotation. They are $\in \mathcal{C}^1$ and have the same return value interval, as well.

4.5 Ground reaction forces and simulation of the sole

The GRFs on the heel and metatarsal-heads MP, 1T, 2T, 3T, 4T und 5T are measured via force platform by Scott and Winter. The calculated curves are given in their paper from 1993. They were scanned and interpolated as cubic splines like the rotation graphs before. In order to always create a force in the direction of the z-axis during the simulation the forces were rotated equal to the torsion of the segments.

Scott and Winter simulate the soft tissue, which transfers force from the ground to the bones / metatarsal heads, with a non-linear spring and a non-linear damper in parallel for each contact point. “The force, F_p, transferred by the tissue was defined by the equation

$$F_p = j\varepsilon^k + l\varepsilon^m | dt\_\varepsilon |^n$$

where j and k define spring and l, m and n define the damper characteristics.” [9] Furthermore, ε stands for the strain, dt_ε for the strain rate. Valiant (1984) supplies a graph, which describes the strain of the heel pad depending on the actual GRF (Figure 4.5.1). Furthermore, Scott and Winter approximate the force-deformation-characteristics of the metatarsal bones and toes by the one of the heel.

To guarantee that all loads at the loading sites can be simulated adequately, the curve with a maximal load of 455 Nm (see Figure 4.5.1) was approximated by splines. Thereby it was divided in two curves: one for compression, the other for decompression. Now the resulting curves were linear scaled regarding their area and thickness of the loading site, as well as their maximal load. These estimated values are listed in table 4.5.1.

If a local maximum in the curve of a GRF appears during the simulation, for the following decompression phase a curve will be supposed, which adopts the local maximum as maximal load for its linear interpolation. The strain of a later compression will be calculated with the proper curve. In this way jumps in the curve of the transferred force are minimized as far as possible.

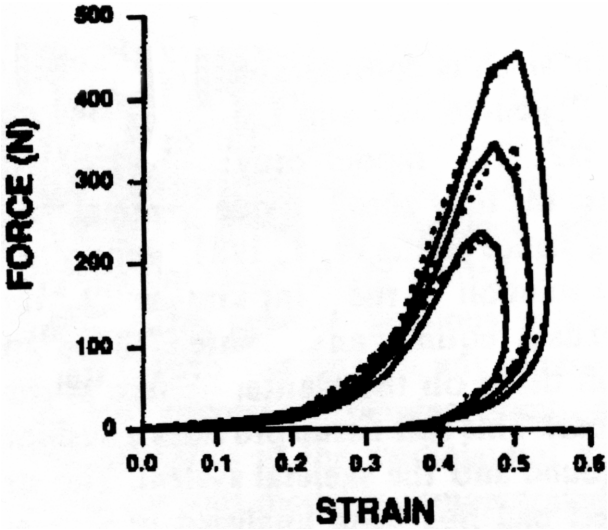

Fig. 4.5.1 mechanical response of the human heel pad for three different maximal impacts

Table 4.5.1 estimated maximal GRFs, thicknesses and areas of the loading sites

Ground contact point	max. GRF	thick (cm)	area (cm²)
TCN	442,35	1,8	19,6
1T	37,43	1,3	12,6
2T	146,70	1,3	7,1
3T	165,40	1,3	7,1
4T	154,96	1,3	7,1
5T	180,25	1,3	7,1
MP	92,16	0,5	7,1

5 The implemented model in C++

5.1 Design of the model

In order to simplify the C++-implementation and to have an additional option to validate orientation and position of the joints and segments the model was premodeled in Matlab. Diagram 5.1.1 includes all connection points, all axes and the approximated cuboids of the talus, calcaneus, and middle-foot-bones.

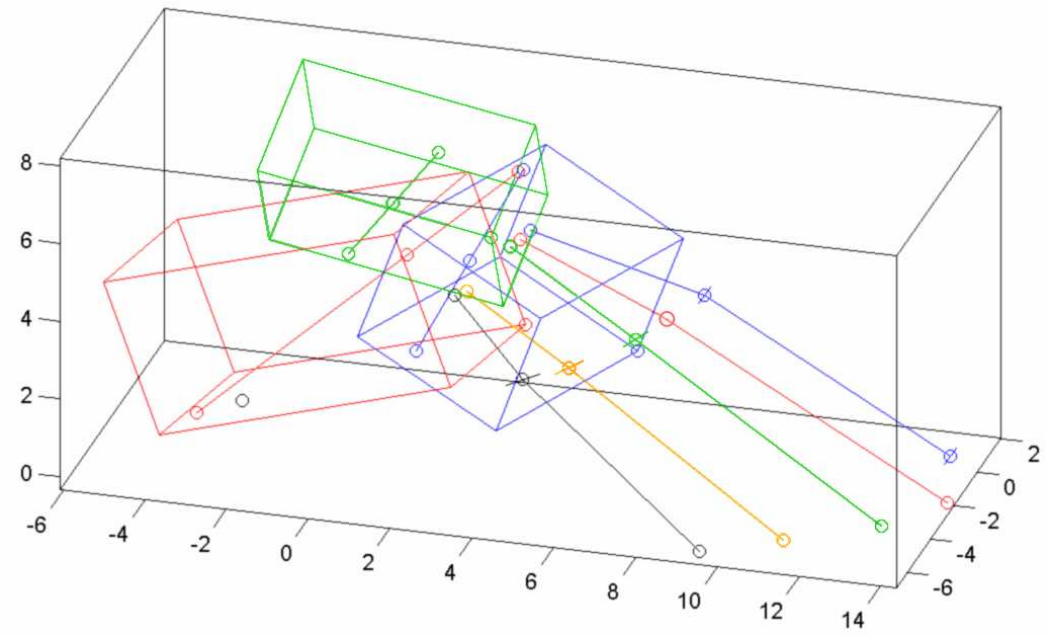

Fig. 5.1.1 the complete foot in Matlab

As the model is constructed traversially in the C++-program it was advantageous to draw a diagram first. The class of segments – “Linkdynamik” – includes just one vector to exact one following segment. Therefore one needs additional segments without mass or inertia, which point from one joint to the next if one or more branches are necessary. These are the segments TT_TCN, 2T_5T, 2T_4T, 2T_3T, and 2T_1T. The model is shown below as a tree (figure 5.1.2).

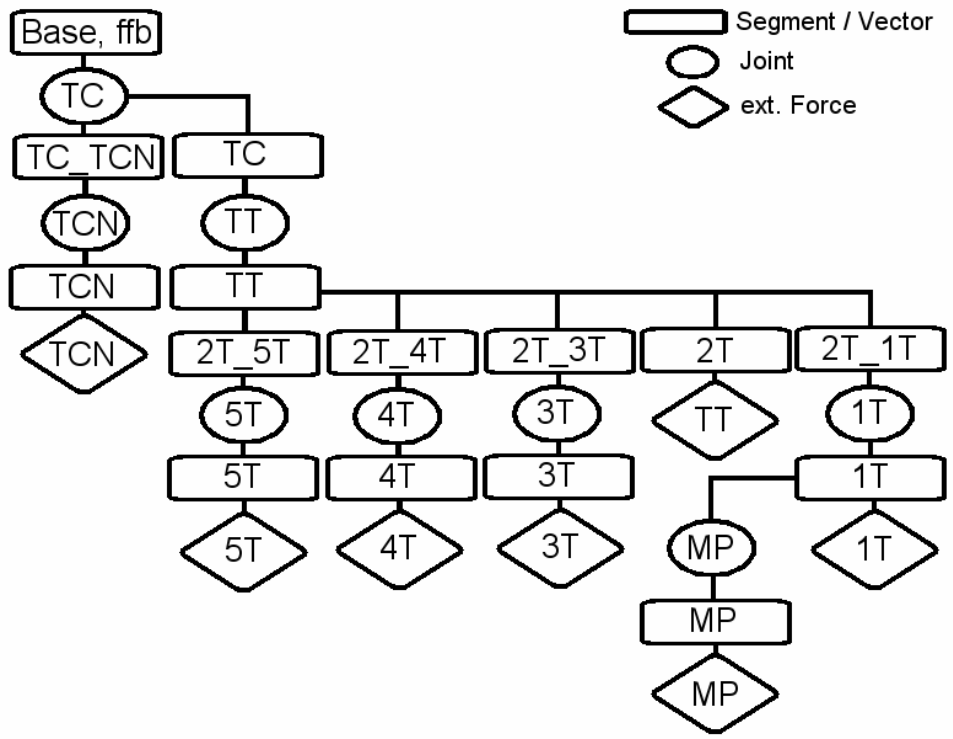

Fig. 5.1.2 schematic diagram of the foot model

5.2 Validation

In order to validate the model using ABA there are generally two possibilities. First it is possible to extract on the hand plots of the second derivative of the joint rotations and on the other hand plots of the acceleration of the angles of rotation from the simulation. In that process joint moments and GRFs are putted on. Despite possibly different orders of magnitudes the general course should be similar. The second available option is to simulate angular accelerations and torques and to compare the resulting forces on the loading sites with the graphs from Scott and Winter. The latter option was dismissed because it does not conform to the original functionality of the model

The model was altered slightly in the validation phase. This included the implementation of a sole with spring- / damper properties (as described in chapter 4.5) as well as an assimilation of the inertia tensors of the segments due to their torsion regarding the coordinate system of the base.

5.3 Results

The following plots are acceleration diagrams with respect to altering simulation conditions. I use the MP-joint for comparing, because the second derivative of its rotations function shows a striking curve (plotted in figure 5.3.3). The corresponding graph of rotation can be seen in diagram 5.3.1, the first derivative in figure 5.3.2.

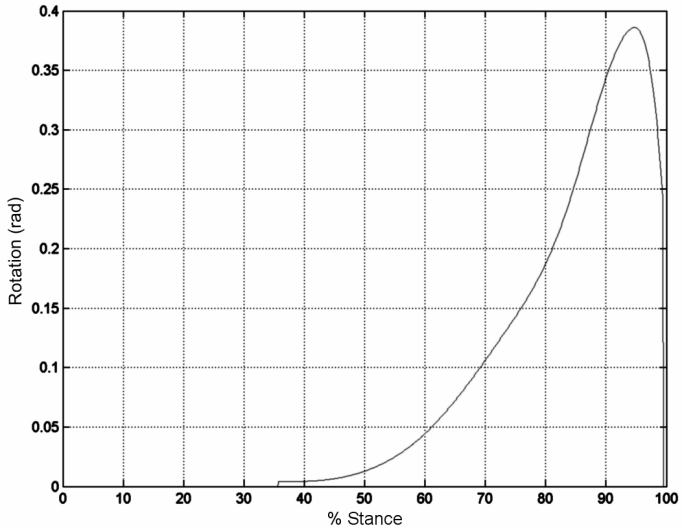

Fig. 5.3.1 rotation curve for the MP-joint (Scott and Winter)

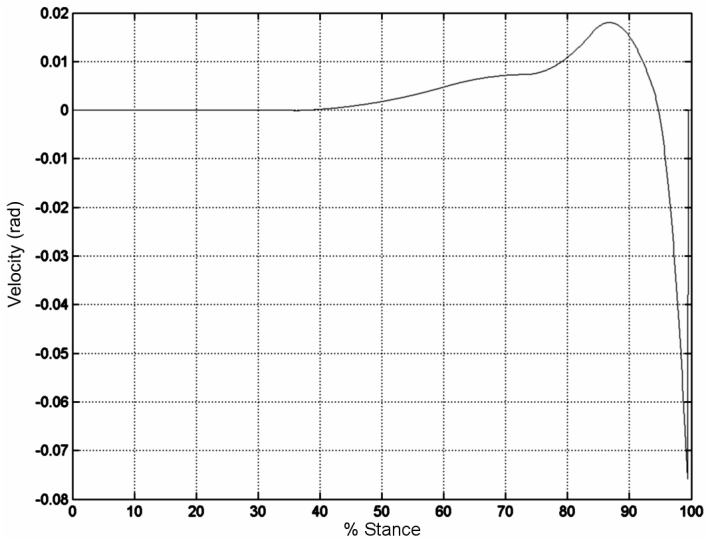

Fig. 5.3.2 first derivative of the rotation curve (Fig. 5.3.1)

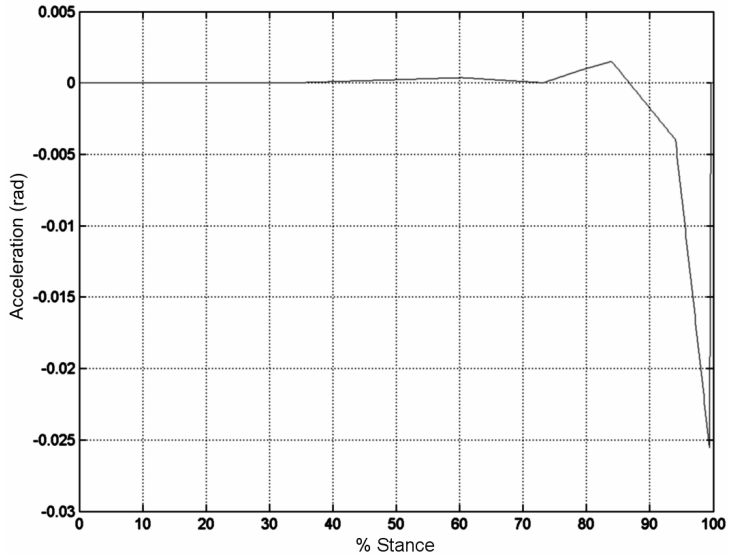

Fig. 5.3.3 second derivative of the rotation curve (Fig. 5.3.1)

For the following simulations earth gravity takes effect in principle. Figure 5.3.4 shows the function for the acceleration of the MP-joint if one leaves joint moments and GRFs out of consideration. The jump at 93% cannot be explained so far but holds a certain significance. Apart from this the similarities with diagram 5.3.3 are obvious. If this run is to be maintained, joint moments, external forces and the weight of the body have to nullify each other.

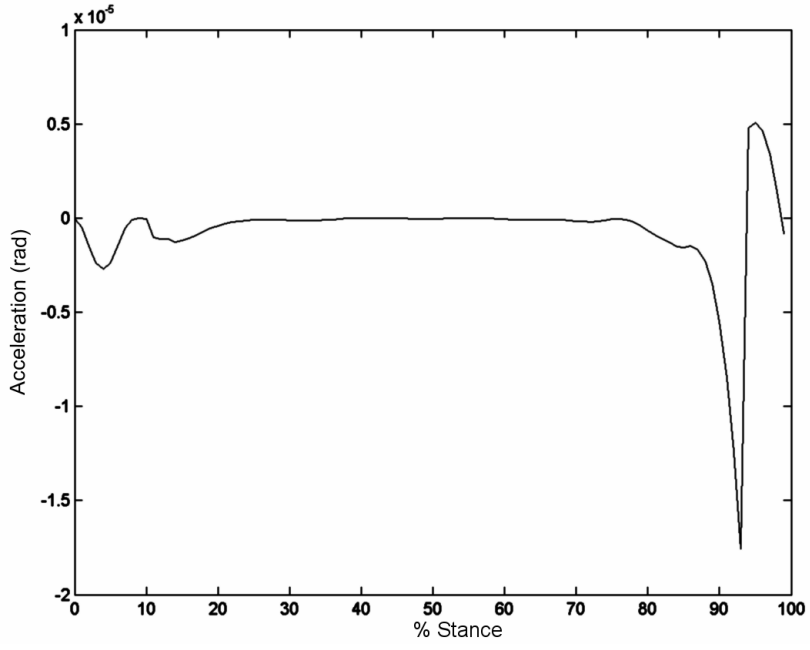

Fig. 5.3.4 acceleration due to rotation and velocity

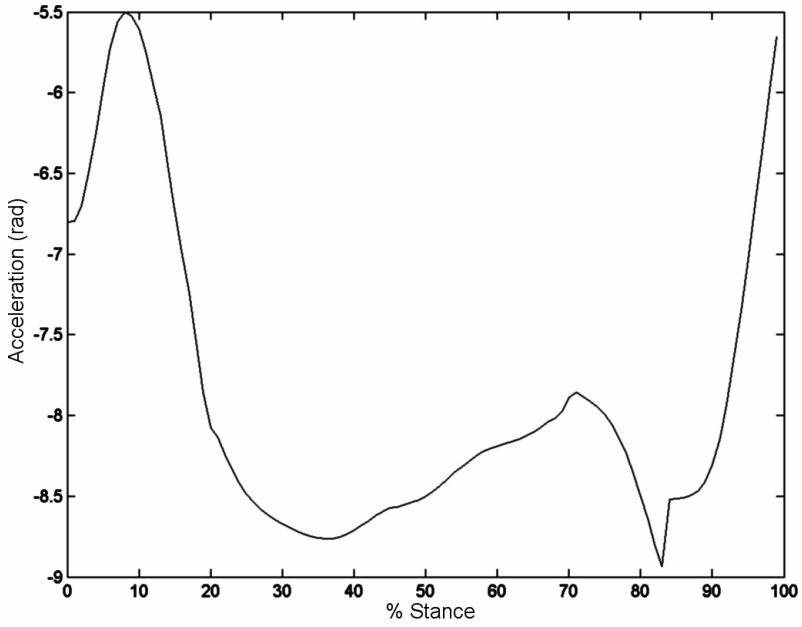

Fig. 5.3.5 acceleration due to body weight and GRFs with sole

For following simulations joint rotation and joint velocity are used in principle. Diagram 5.3.5 shows several typical effects and properties of the specific components used in this simulation. The influence of the body weight accounts for the y-intercept smaller than zero. Here at approximately -6.7. The graph is almost consistently continuous and the difference between maximal and minimal acceleration is due to the use of the sole relatively small. Here approximately 3.4.

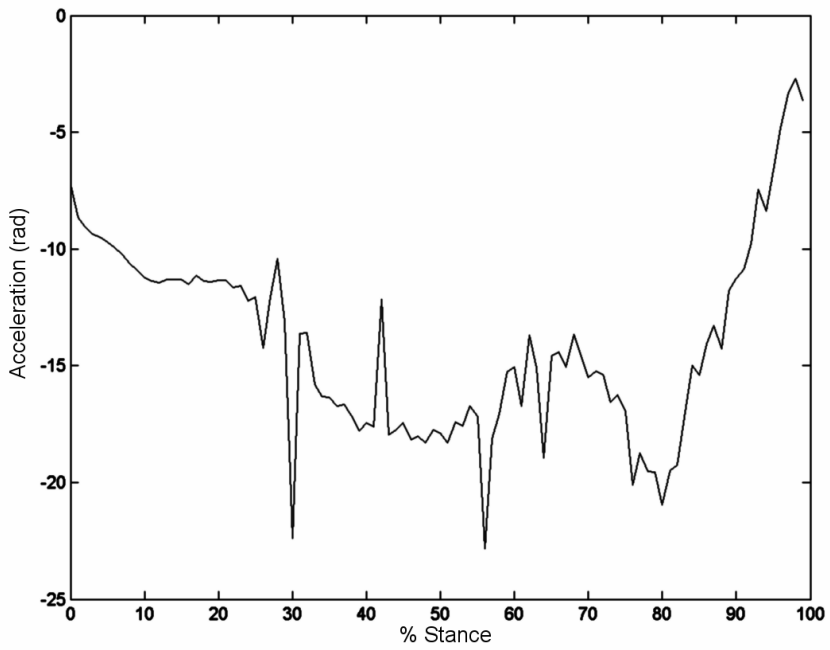

Fig. 5.3.6 acceleration due to body weight, GRFs without sole, and joint moments

Diagram 5.3.6 shows the joint acceleration for active body weight, GRFs without soft tissue modelling and joint moments. The jagged run is caused by the moments. The difference of about 17 (in relation to the magnitude) is close to the difference of the expected acceleration in diagram 5.3.3, where it is about 0.027.

5.4 Summary and perspective

The graph in the diagram 5.3.6 does not yield the wanted run from 5.3.3. The other joints show similar results. There are a couple of possible reasons for this discrepancy. For one thing a lot of lengths and contact points were merely approximated or read off sketches. Sometimes data from different sources was combined for example in the case of rotation axes. The resulting model is a product of varying mathematical needs and deductions. Only a few coordinates were given for the positions of the joints and even these were approximated for mathematical simplicity. Therefore, more specific positions of the bones are a possible improvement of this model.

Moreover, a point is a correct modelling of the ground contact. This has not been described properly by using GRFs. Displacement of the contact points by forward drift, torsion of the contact points by foot spin, and so on were not modelled yet. At this point in-depth-studies are required.

The mathematics of the ABA transports completely forces and torques from the other segments to the attached segments. This procedure certainly needs to be refitted to be able to simulate human joints, because natural joints are not rigid. Every joint needs to contain additional damper characteristics. Diagram 5.3.6 shows that GRFs and joint moments of other segments and joints have such a lot of influence on the last element in the chain, that the process of acceleration is quite different to the expected graph. The acceleration values of the TC joint lie predominantly between -10^{19} und 10^{19}. Whether this magnitude of scale is caused by the summation of all adjacent forces of the other segments or also by a model fault, could not be determined. A visualisation of the model by the C++-program could give feedback whether the problem lies within the construction of the model. Though, this is impossible at the moment.

A model was developed that comes close to the anatomy of human feet. Every important joint is modelled adequately; all important segments are approximated by cuboids or hollow cylinders. The general idea to use external forces as GRFs and internal moments as muscles has led to proper results even if they do not show the wanted run. Because the model does not contain advanced mathematical principles, it will be easy to understand it from an outsider's point of view to optimize it or adapt it to the needs of specific simulations. It appears to me, because of this and the reasons shown above, that it can be used as a good foundation for simulations of human locomotion in future.

6 References

[01] Gilchrist, L.A. and Winter, D.A.
(1996), *A two-part viscoelastic foot model for use in gait simulations*, Journal of Biomechanics **29**, No. 6, 795-798

[02] Günther, Michael (1997), *Computersimulation zur Synthetisierung des muskulär erzeugten menschlichen Gehens unter Verwendung eines biomechanischen Mehrkörpermodells*, vorgelegt Frankfurt/Main

[03] Henze, Arnim (2002) *Dreidimensionale biomechanische Modellierung und die Entwicklung eines Reglers zur Simulation zweibeinigen Gehens*

[04] Hicks, J.H. (1954), *The mechanics of the foot: II. The plantar aponeurosis and the arch*, Journal of Anatomy **88**, 25-31

[05] Morlock, M. M. (1989), *A generalized three-dimensional six-segment model of the ankle and the foot*, Unpublished doctoral dissertation, University of Calgary, Calgary, Alberta, Canada

[06] Platzer, Werner (1999), *Taschenatlas der Anatomie, Bewegungsapparat,* 7. Auflage, Georg Thieme Verlag Stuttgart

[07] Salathé et al., E.P. Jr. Arangio, G.A. and Salathé, E.P
(1986), *A biomechanical model of the foot*, Journal of Biomechanics **19**, No. 12, 989-1001

[08] Scott, S.H. and Winter, D.A.
(1991), *Talocrural and talocalcaneal joint kinematics and kinetics during the stance phase of walking,* Journal of Biomechanics **24**, 742-752

[09] Scott, S.H. and Winter, D.A.
(1993), *Biomechanical model of the human foot: kinematics and kinetics during the stance phase of walking,* Journal of Biomechanics **26**, No. 9, 1091-1104

[10] http://www.auburn.edu/academic/classes/hlhp/3620/PHASE_2/Ankle Lecture.ppt

Appendix - CD